

Mixing with the radio frequency single-electron transistor

L. J. Swenson,^{a)} D. R. Schmidt, J. S. Aldridge, D. K. Wood, and A. N. Cleland
Department of Physics, University of California at Santa Barbara, Santa Barbara, California 93106

(Received 20 September 2004; accepted 16 March 2005; published online 21 April 2005)

By configuring a radio frequency single-electron transistor as a mixer, we demonstrate a unique implementation of this device, that achieves good charge sensitivity with large bandwidth about a tunable center frequency. In our implementation we achieve a measurement bandwidth of 16 MHz, with a tunable center frequency from 0 to 1.2 GHz, demonstrated with the transistor operating at 300 mK. Ultimately this device is limited in center frequency by the RC time of the transistor's center island, which for our device is ~ 1.6 GHz, close to the measured value. The measurement bandwidth is determined by the quality factor of the readout tank circuit. © 2005 American Institute of Physics. [DOI: 10.1063/1.1923188]

In mesoscopic experiments requiring ultrasensitive charge detection, the single-electron transistor (SET) has become widely recognized as one of the most suitable charge amplifiers. With the experimental realization by Fulton and Dolan,¹ and theoretical description by Averin and Likharev,² the SET is a small-capacitance metallic island onto and off of which electrons can tunnel via source and drain leads. At low temperatures $k_B T \ll e^2/2C_\Sigma$, where C_Σ is the island capacitance, tunneling is suppressed for source-drain voltages V in the range $|V| < e/2C_\Sigma$, known as the Coulomb blockade. By introducing a gate lead, capacitively coupled to the metallic island, the electrostatic energy of the island, and hence the tunneling rate, can be manipulated by voltages on the gate. The drain-source current is extremely sensitive to the gate charge, yielding a very low noise charge-to-current transducer. Successful operation of the SET requires that the tunnel resistance R_T of the drain and source junctions satisfy $R_T \geq R_K = h/e^2 \approx 25.8$ k Ω , the quantum of resistance.

Despite its clear advantages, the SET has until recently suffered from a major drawback: The large tunnel resistance R_T , coupled with the unavoidable stray capacitance of the wiring, $C_{\text{stray}} \sim 10^{-12}$ F, limits the output bandwidth to at best $1/2\pi R_T C_{\text{stray}} \sim 1$ –10 MHz. High frequency signals, necessary for measurement of the dynamics of systems such as a nanomechanical resonator³ or an excited Cooper-pair box,⁴ remain undetected when operating with the standard SET configuration. Two recent innovations have demonstrated significant improvements on this limiting behavior, greatly increasing the SET's spectral range. The first approach was to use a series inductance, resonating with the stray lead capacitance, to create a tank circuit that roughly impedance matches the SET to a low-impedance cable. This innovation is termed the radio frequency single-electron transistor, or rf-SET,⁵ and has been used to achieve measurement bandwidths in excess of 100 MHz, with intrinsic charge noise below $10^{-5} e/\sqrt{\text{Hz}}$.⁶ The second approach was to use the nonlinear response of the SET current to the gate signal to implement the SET as a radio frequency mixer, still limited by the RC charging time to a narrow bandwidth, but allowing measurements at center frequencies tunable up to 1–10 GHz, limited by the intrinsic $1/RC_\Sigma$ bandwidth of the SET island.⁷

Here we demonstrate experimentally that the large bandwidth of the rf-SET, and the tunability of the SET mixer, can be simultaneously achieved. A schematic of the measurement setup is shown in Fig. 1. An all-aluminum SET, with a total tunneling resistance $R_T \approx 95$ k Ω , island capacitance $C_\Sigma \approx 550$ aF, and input gate capacitance $C_g \approx 22$ aF, was fabricated by standard shadow evaporation on a semi-insulating GaAs chip. The chip was glued to a printed circuit board mounted in a metal box, and mounted on the cold stage of a 300 mK ³He cryostat. The source of the SET was grounded and the drain lead was connected in series with a 390 nH inductor, in a standard rf-SET configuration; the resonant capacitance is mostly that of the on-chip drain lead to the SET. The other end of the inductor was connected to a 50- Ω semirigid coaxial cable, interrupted by a bias tee for applying dc bias power, before passing out of the cryostat to room-temperature electronics. This configuration gave a resonant tank circuit frequency $f_{LC} = 326$ MHz. A second 50- Ω coaxial cable was connected to the gate of the SET, interrupted by a bias tee to allow dc voltages to tune the operating point of the SET.

By applying a dc bias to the drain, and measuring the power reflected at the carrier frequency f_c from the tank circuit, set to the tank circuit resonance frequency $f_c = f_{LC}$, the device was first operated as a rf-SET in the superconducting state.⁸ In this implementation, a dc gate voltage V_0 , and a rf gate signal V_s at frequency f_s , modulates the SET

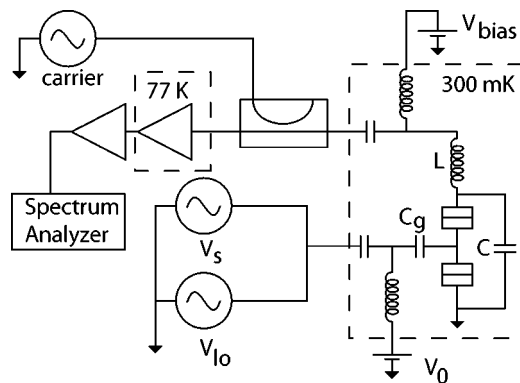


FIG. 1. Schematic of the measurement circuit. The dashed outline shows cryogenic part of experiment, and L and C indicate the tank circuit elements; C_g is the SET gate capacitance. V_s and V_{I_0} are rf signal amplitudes; V_0 is the dc gate bias. The reflected power preamplifier is cooled to 77 K.

^{a)}Electronic mail: lswenson@physics.ucsb.edu

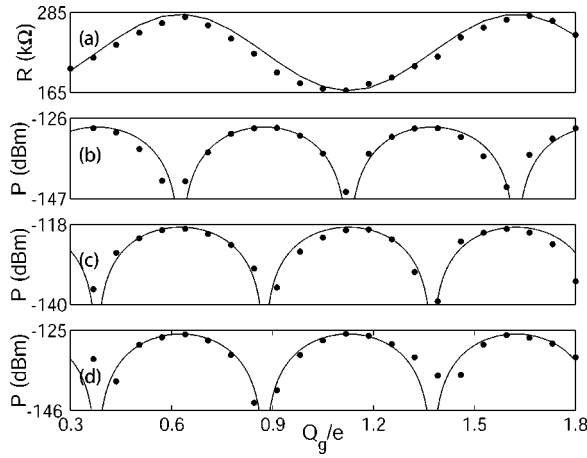


FIG. 2. SET response as a function of the dc gate charge: (a) the drain-source differential resistance $\Delta R = dV/dI(Q_g) - dV/dI(0)$; the solid line is a sinusoidal fit. (b) First harmonic reflected power, with a 0.5 MHz, $0.01e$ amplitude rf signal applied to the gate (small amplitude limit). (c) Second harmonic reflected power, with a 0.5 MHz, $0.09e$ large-amplitude rf signal on the gate. (d) Reflected power of heterodyne mixer at the sideband $|f_{10} - f_s|$, where $f_{10} = 412$ MHz and $f_s = 410$ MHz. $C_g V_{10}$ and $C_g V_s$ were held fixed at $0.19e$ and $0.15e$, respectively.

differential drain-source resistance, and thus modulates the reflected power amplitude. As the drain-source resistance modulation ΔR was always very small, the reflection coefficient is to a good approximation linearly dependent on ΔR . The resistance modulation is a function of the gate voltage, $V_g = V_0 + V_s \cos(2\pi f_s t)$. Figure 2(a) shows the measured dependence of ΔR on the gate charge $Q_g = C_g V_0$, with no applied rf signal. We operated at a bias point, near the Josephson quasiparticle peak, where the SET drain-source differential resistance change $\Delta R = dV/dI(Q_g) - dV/dI(0)$ has a sinusoidal dependence on the gate charge,

$$\Delta R \approx R_g \cos\left(\frac{2\pi Q_g}{e}\right), \quad (1)$$

where R_g is the range accessible by gating around the constant value $dV/dI(0)$. A fit of Eq. (1) to the data is displayed in Fig. 2(a). Using this approximation, the time-dependent resistance change of the SET, with a rf signal at the gate, is given by

$$\Delta R(t) \approx R_g \cos\left(\frac{2\pi C_g}{e} [V_0 + V_s \cos(2\pi f_s t)]\right). \quad (2)$$

For small rf amplitudes $C_g V_s \ll e$, with the gate dc bias V_0 chosen so that Eq. (2) has the steepest slope, at, e.g., $C_g V_0 = -e/4$, the SET resistance change is linear in the gate amplitude. For these small resistance changes, the spectrum of the power reflected from the tank circuit contains two sidebands at $f_c \pm f_s$, whose amplitudes are also linearly dependent on the rf gate amplitude $C_g V_s$; this is the usual mode of operation for the rf-SET.

For larger gate amplitudes, the SET resistance becomes nonlinearly related to the gate signal, and the reflected power spectrum then contains additional sidebands at $f_c \pm n f_s$, where n takes on positive integer values. The strength of the harmonic terms depends nonlinearly on the gate signal amplitude, as well as on the gate dc bias point.

In Figs. 2(b) and 2(c) we show the measured sideband reflected power as a function of the gate charge $C_g V_0$ for the $n=1$ and $n=2$ harmonics, with signal amplitude V_s fixed at

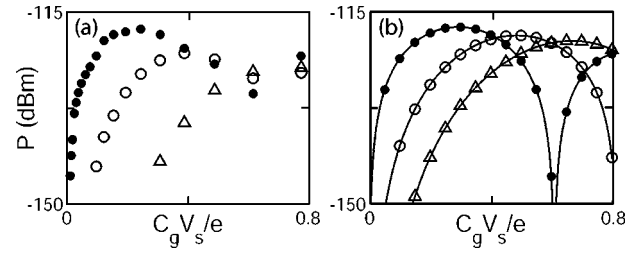


FIG. 3. Reflected power as a function of rf gate amplitude $C_g V_s$: (a) The measured sideband reflected power for the first (\bullet), second (\circ), and third (\triangle) harmonics, as a function of $C_g V_s$, ranging from 0 to $0.8e$. The gate rf signal was at 4 MHz. (b) Model dependence for the first (\bullet), second (\circ), and third (\triangle) sideband reflected power, under the same conditions as (a).

$0.01e$ and $0.09e$, respectively. As can be seen by comparing to Fig. 2(a), the $n=1$ and, in general, the odd harmonics give maximum amplitude when the dc gate charge is adjusted to put Eq. (1) at a point of steepest slope, while the $n=2$ and even harmonics are maximized when the gate charge puts Eq. (1) at an extremum.

In Fig. 3(a) we show the dependence of the reflected power for the first three harmonics on the rf gate amplitude V_s . As noted above, the odd harmonics were measured at $C_g V_0 = e/4$ and the even harmonics at $C_g V_0 = e/2$. To model this dependence, we Fourier transform Eq. (2) for each harmonic. The Fourier coefficients for $n \leq 3$ can be expressed by

$$c_n = \left| R_g J_n \left(\frac{2\pi C_g V_s}{e} \right) \right|, \quad (3)$$

where J_n is the n th order Bessel function. In Fig. 3(b) we show the model rf-SET response for the first three harmonics, equal to $20 \log_{10}(c_n)$ plus an offset that depends on the overall reflection coefficient and incoming power level. Agreement is relatively good.

The response we have described so far represents a form of homodyne detection with the rf-SET. However, the nonlinear response of the SET differential resistance to the gate charge allows the rf-SET to also be used as a heterodyne mixer, sensitive to *small* signal variations on the gate. This is achieved by applying a large-amplitude local oscillator (LO) to the gate at frequency f_{10} , in addition to the small signal to be detected at frequency f_s . With both signals applied to the SET gate, the SET resistance response can be modeled using the approximate response given by Eq. (1),

$$\Delta R \approx R_g \cos\left(\frac{2\pi C_g}{e} [V_0 + V_{10} \cos(2\pi f_{10} t) + V_s \cos(2\pi f_s t)]\right), \quad (4)$$

where V_{10} and V_s are the local oscillator and signal amplitudes, respectively.

In the nonlinear response regime of the SET, the resistance change given by Eq. (4) contains frequency components f_{mn} , where $f_{mn} = |m f_{10} \pm n f_s|$, for positive integers m and n . For either m or n equal to zero, this is the previously described homodyne detection. The spectrum of the power reflected from the SET tank circuit then has components $f_c \pm f_{mn}$ about the carrier frequency f_c . A Fourier representation of Eq. (4) thus contains an infinite number of terms with nonzero coefficients; we only consider those within the output bandwidth of the rf-SET. For small rf signal amplitude

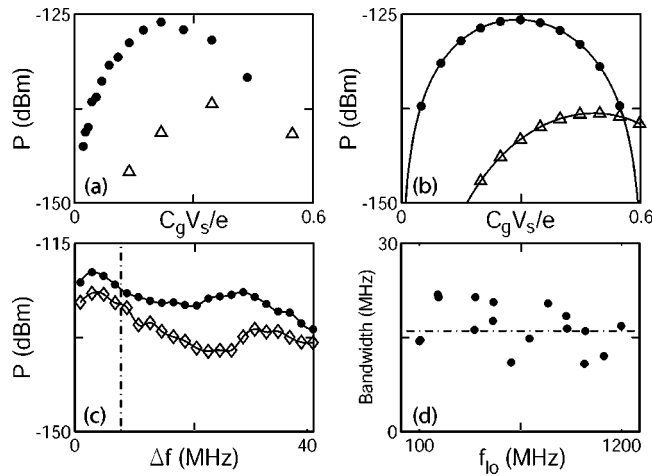


FIG. 4. Characterization of the rf-SET heterodyne response, as a function of gate charge and frequency. (a) Measured sideband reflected power for sidebands $|f_{l0} - f_{s1}|$ (\bullet) and $|2f_{l0} - 2f_{s1}|$ (Δ) as a function of $C_g V_s$, which ranges from 0 to $0.6e$. $C_g V_{l0}$ was held fixed at $0.17e$, the dc gate bias was set optimally, $f_{l0} = 410$ MHz, and $f_s = 412$ MHz. (b) Modeled sideband reflected power under the same amplitude conditions as in (a). (c) First harmonic reflected power as a function of frequency separation Δf from f_c . For homodyne detection (\bullet), $\Delta f = |f_{s1}|$, and when operated as a mixer (\diamond), $\Delta f = |f_{l0} - f_s|$ where $f_{l0} = 400$ MHz. The dashed line is 3 dB down from the maximum reflected power, yielding a 16 MHz bandwidth. (d) Measured mixer bandwidth as a function of f_{l0} . The dashed line is at 16 MHz.

V_s , the Fourier coefficients will be most appreciable for m , $n \leq 2$. When $m+n$ is even, the Fourier coefficient is a maximum when the resistance change ΔR given by Eq. (1) is at an extremum; when $m+n$ is odd, the coefficient is greatest when the derivative of ΔR with respect to the gate charge is maximized. The case for $|f_{l0} - f_{s1}|$ ($m=n=1$, $m+n$ even) is shown in Fig. 2(d).

Using our model, under optimal dc bias conditions the Fourier coefficients for m , $n \leq 2$ can be expressed as

$$c_{mn} = \left| R_g J_m \left(\frac{2\pi C_g V_{l0}}{e} \right) \times J_n \left(\frac{2\pi C_g V_s}{e} \right) \right|. \quad (5)$$

In Fig. 4(a) we show the measured dependence of the reflected power sideband components $m=n=1$ and $m=n=2$ on $C_g V_s$, with a dc gate bias optimized separately for each component. In Fig. 4(b) we show the model response, equal to $20 \log_{10}(c_{mn})$ plus an offset, in fairly good correspondence with Fig. 4(a). In Fig. 4(c) we show the dependence of the first harmonic reflected power on frequency separation from f_c , for both homodyne and heterodyne detection. In Fig. 4(d) the mixer bandwidth as a function of f_{l0} is displayed.

For both homodyne and heterodyne detection, the first harmonic ($n=1$) yields the greatest charge sensitivity for small signals V_s . When operated as a mixer, the charge sensitivity is maximized when $m=1$ (first LO component) and $C_g V_{l0} \sim 0.293e$ (maximum of the Bessel function corresponding to the LO signal). However, due to the form of c_{mn} , the signal when mixing will be reduced by about 5 dB compared to homodyne detection.

We have measured the charge sensitivity of this device, operating both as a rf-SET and as a heterodyne mixer. The calculation of charge sensitivity for the rf-SET has been previously published.^{5,10} The charge noise for optimal bias conditions was measured to be $\delta q_s \leq 2 \times 10^{-3} e / \sqrt{\text{Hz}}$ in rf-SET mode, and increased slightly to $\delta q_s \leq 5 \times 10^{-3} e / \sqrt{\text{Hz}}$ when operated as a mixer. However, these values were dominated by the noise in the 77 K preamplifier, used to amplify the reflected power from the tank circuit; a 4.2 K mounted preamplifier would likely yield better noise figures.⁵ These indicate that the performance of the rf-SET when used as a mixer is not significantly worse than when used in homodyne detection.

In conclusion, we have demonstrated mixing with a rf-SET, allowing tuning of the 16 MHz measurement bandwidth around a center frequency which could be set up to 1.2 GHz. The center frequency is ultimately limited by the RC time constant of the SET center island, here estimated to give a limit of $1/2\pi RC \sim 1.6$ GHz. This technology will facilitate transmission-style measurements requiring both small signal detection and sensitivity over a broad range of signal frequencies and amplitudes.

We thank Bob Hill for processing support, and we acknowledge financial support provided by the NASA Office of Space Science under Grant No. NAG5-11426.

¹T. A. Fulton and G. J. Dolan, Phys. Rev. Lett. **59**, 109 (1987).

²D. V. Averin and K. K. Likharev, J. Low Temp. Phys. **62**, 345 (1986).

³R. G. Knobel and A. Cleland, Nature (London) **424**, 291 (2003).

⁴K. W. Lehnert, K. Bladh, L. F. Spietz, D. Gunnarsson, D. I. Schuster, P. Delsing, and R. J. Schoelkopf, Phys. Rev. Lett. **90**, 027002 (2003).

⁵R. J. Schoelkopf, P. Wahlgren, A. A. Kozhevnikov, P. Delsing, and D. E. Prober, Science **280**, 1238 (1998).

⁶M. H. Devoret and R. J. Schoelkopf, Nature (London) **406**, 1039 (2000).

⁷R. Knobel, C. S. Yung, and A. N. Cleland, Appl. Phys. Lett. **81**, 532 (2002).

⁸T. A. Fulton, P. L. Gammel, D. J. Bishop, L. N. Dunkleberger, and G. J. Dolan, Phys. Rev. Lett. **63**, 1307 (1989).

⁹A. Aassime, D. Gunnarsson, K. Bladh, P. Delsing, and R. Schoelkopf, Appl. Phys. Lett. **79**, 4031 (2001).

¹⁰L. Roschier, P. Hakonen, K. Bladh, P. Delsing, K. W. Lehnert, L. Spietz, and R. J. Schoelkopf, J. Appl. Phys. **95**, 1274 (2004).